ISJ 17: 147-162, 2020 ISSN 1824-307X

RESEARCH REPORT

# Hemocyte profile, phagocytosis, and antibacterial activity in response to immune challenge of the date fruit stalk borer, *Oryctes elegans*

**MY Al Mutawa[1], TH Ayaad[2], EH Shaurub[2]***

*[1]Department of Zoology, Faculty of Science, King Saud University, Saudi Arabia*
*[2]Department of Entomology, Faculty of Science, Cairo University, Giza, P.O. Box 12613, Egypt*

 *Accepted July 07, 2020*

## Abstract

The date fruit stalk borer, *Oryctes elegans* Prell, is a destructive pest on date palms in Saudi Arabia. We evaluated the immune response of the third instars (last instars), by the intrahemocoelic injection of lipopolysaccharide (LPS) (a pathogen-associated molecular peptide, PAMP), which significantly increased the total hemocyte count. Phase-contrast light microscopy revealed the presence of five hemocyte types: prohemocytes, granulocytes, plasmatocytes, oenocytoids ,and spherulocytes. Transmission electron microscopy demonstrated that, among these hemocytes, only the granulocytes and plasmatocytes phagocytosed latex beads. Injection with LPS also significantly decreased the number of oenocytoids. The antibacterial activity of plasma proteins of larvae injected with LPS, measured using the agar well diffusion method, against Gram-positive and Gram-negative bacteria varied based on the bacterial strain, the total concentration of plasma protein, and time post-injection with LPS. The results of the current study may be useful in the biological control of *O. elegans*. Furthermore, new compounds with antibacterial activity that might be useful for the development of innovative drugs of natural origin can be identified in *O. elegans*.

**Key Words**: *Oryctes elegans*; total hemocyte count; differential hemocyte count; hemocyte morphology; phagocytosis; antibacterial activity

## Introduction

Date palm (*Phoenix dactylifera* L.) (Arecales: Arecaceae) is one of the most economically important fruit trees in Saudi Arabia and they cover approximately 155,118 ha and produced 991,546 tons of fruit in 2011 (Al-Ayedh and Al Dhafer, 2015). The date fruit stalk borer, *Oryctes elegans* Prell (Coleoptera: Scarabaeidae), is a destructive pest on *P. dactylifera* in Saudi Arabia and many other places globally (Latifian and Rad, 2012; Al-Ayedh and Al Dhafer, 2015; Bedford *et al*., 2015). Adults of *O. elegans* bore tunnels into the stalks of fruit bunches to feed, causing them to break off during windstorms. Females oviposit in leaf axils and groups of larvae may tunnel inside the trunk causing the palm to topple (Bedford *et al*., 2015). Moreover, there have been indications that the feeding sites of *O. elegans* larvae may predispose palm trees to oviposition by the females of the red palm weevil, *Rhynchophorus ferrugineus* (Olivier) (Coleoptera: Curculionidae) (Al-Ayedh and Al Dhafer, 2015).

Since *O. elegans* is a concealed tissue borer, it is difficult to detect symptoms of its attack at an early stage of infestation. Therefore, preventative measures are applied to manage *O. elegans*, which include physical control, trapping, host plant resistance, quarantine measures, and biological control (Latifian and Rad, 2012; Bedford *et al*., 2015; Atwa, 2018). The development of a biological control strategy for the successful integrated management of *O. elegans* requires the identification of its pathogens and more in-depth information about its immune system and defensive mechanisms against its pathogens.

The immune response in insects differs fundamentally from that of vertebrates in the lack of cell specificity, immunoglobulins, and response memory. However, similar responses to immune memory in insects have been described as a phenomenon called "immune priming," where the insect exposed to a low dose of a pathogen becomes more resistant when later exposed to a high dose of the same pathogen (Gálvez and Chapuisat, 2014; Sheehan *et al*., 2020). The innate immune system of insects consists of physical barriers, including the exoskeleton and peritrophic

*Corresponding author:*
EH Shaurub
Department of Entomology
Faculty of Science
Cairo University
Giza, P.O. Box 12613, Egypt
E-mail: shaurub@sci.cu.edu.eg

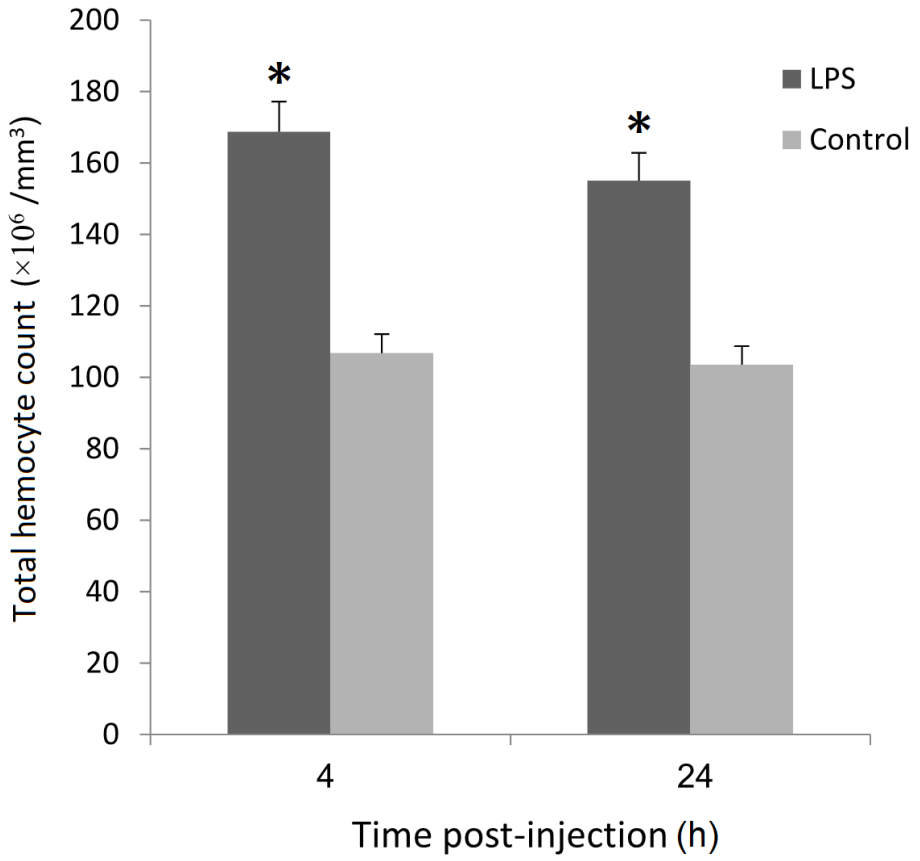


**Fig. 1** Total hemocyte count of *O. elegans* third instars 4 h and 24 h post-injection with lipopolysaccharide (LPS). Data are presented as the mean ± SE. *, Significant at $p < 0.05$ compared to the control, using Student's *t*-test

membrane, cellular responses, and humoral responses (Lavine and Strand, 2002; Shaurub, 2012; Hillyer and Strand, 2014; Hillyer, 2016). When the barriers are breached, the cellular and humoral immune responses are activated (Lemaitre and Hoffmann, 2007; Hillyer, 2016).

The cellular immune responses are performed by hemocytes and include phagocytosis, nodulation, and encapsulation (Lavine and Strand, 2002; Shaurub, 2012; Browne *et al*., 2013; Hillyer, 2016; Dorrah *et al*., 2019). In most insects, granulocytes and plasmatocytes are the phagocytic cells (Manachini *et al*., 2011; Kwon *et al*., 2014; Zhang and Zhang, 2019).

The humoral immune responses are based on the products of characterized immune genes induced by microbial infection and encode antimicrobial peptides (AMPs), which are synthesized predominantly in fat body and released into hemolymph (Hoffmann, 1995; Gillespie *et al*., 1997; Nakatogawa *et al*., 2009; Shia *et al*., 2009). These genes are either not expressed or are constitutively expressed at a low rate prior to infection (Hoffmann, 1995; Engström, 1998). Insect AMPs could be categorized into the following major groups based on their secondary structure, amino acid sequence and antibacterial activity: linear amphipathic α- helix-forming peptides (e.g. cecropins), β-sheets or cystine-rich and cyclic AMPs (e.g. defensin), and proline-rich peptides and glycine-rich peptides (e.g. drosocin and coleoptericin) (Trenczek et al., 1997; Bulet, 2005; Hull, 2012). The literature has described several coleopteran AMPs (Hall *et al*., 2011; Ntwasa et al., 2012). Among them, cecropins, defensin, and attacins are not peculiar to this insect order, but coleoptericin, rhinocerocin, and holotricin have been described exclusively in Coleoptera (Ntwasa *et al*., 2012). AMPs identified in many insects operate synergistically against a wide range of Gram-positive and Gram-negative bacteria. The onset of these molecules occurs after stimulation of the host with both viable and killed bacteria (Cociancich *et al*., 1994; Brivio *et al*., 2006; Lemaitre and Hoffmann, 2007) but also if larvae are immunized with a purified bacterial pathogen-associated molecular peptide (PAMP) (e.g. lipopolysaccharide, LPS) (Mastore, 2015).

In addition, humoral immune responses include activation of enzymic cascades that regulate coagulation and melanization of hemolymph, and production of reactive oxygen and nitrogen species (ROS-RNS) (Gilespie *et al*., 1997; Bogdan *et al*., 2000; Nappi and Vass, 2001; Hoffmann, 2003; Mavrouli *et al*., 2005; Dorrah *et al*., 2019).

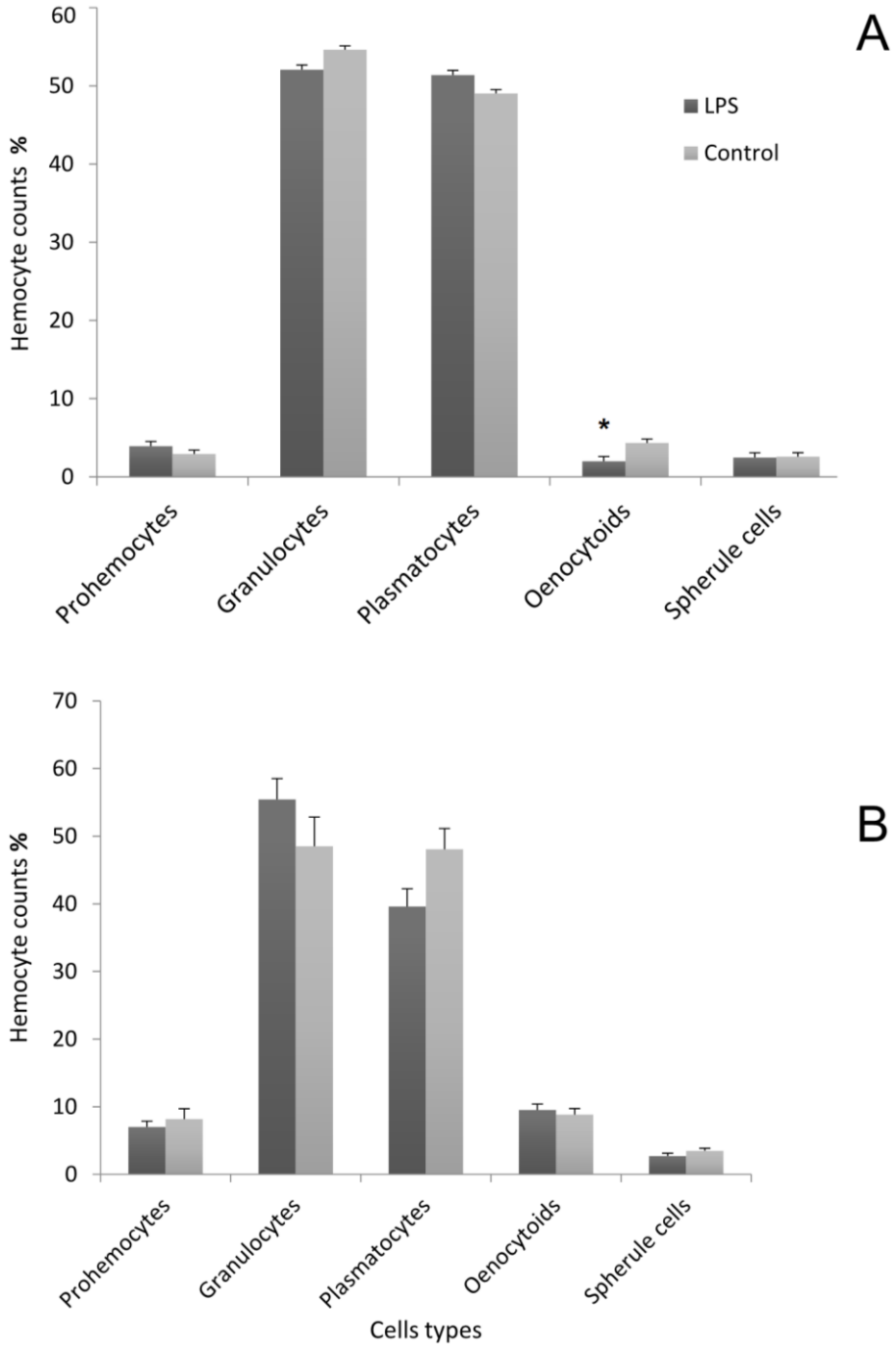


**Fig. 2** Differential hemocyte count of *O. elegans* third instars 4 h (A), and 24 h post-injection (B) with lipopolysaccharide (LPS). Data are presented as the mean ± SE. *, Significant at $p < 0.05$ compared to the control, using Student's *t*-test

Most of the immunological studies on coleopterans that infest palm trees have been conducted on *R. ferrugineus*. For instance, hemocytes counts have been conducted, and phagocytosis (Manachini *et al*., 2011) and antibacterial activity have been reported (Mazza *et al*., 2011; Mastore *et al*., 2015; Sewify *et al*., 2017). However, few immunological studies have been conducted on *Oryctes* spp., except for studies on antibacterial activity (Rabeeth *et al*., 2012; Veeramani *et al*., 2017).

To the best of our knowledge, no studies have been conducted to elucidate the inducible immune response of *O. elegans*. Therefore, this study aimed to elucidate i) total and differential hemocyte counts of third instars of *O. elegans* injected with LPS, ii) *in*

*vivo* phagocytosis by hemocytes of larvae injected with latex, and iii) antibacterial activity of plasma proteins of larvae injected with LPS against three Gram-positive bacteria, *Staphylococcus aureus* Rosenbach (Bacillales: Staphylococcaceae), *Micrococcus luteus* (Schroeter) Cohen (Micrococcales: Micrococcaceae) and *Bacillus subtilis* (Ehrenberg) Cohen (Bacillales: Bacillaceae), and a Gram-negative bacterium, *Escherichia coli* (Migula) Castellani and Chalmers (Enterobacterales: Enterobacteriaceae).

**Materials and methods**

*Sampling*

The mature third instars (last instars) of *Oryctes elegans* averaging 7.61 g in weight, 7.58 cm in length, and 5.23 cm in body circumference were collected during October and November 2012 and 2013 from the trunks of infested date palms in a private organic farm at Ha'il Province, Saudi Arabia (27°11'56"N, 42°59'13"E). The fallen and rotted palm trunks were open up to collect the third instars or they were directly collected underneath such trunks (Atwa, 2018; Pradipta *et al*., 2020). Larvae were transported together with the soft frond bases of date palms in a well-ventilated container to the laboratory at 27 ± 2°C and 65 ± 5 % relative humidity. They were used for the immunological assays within 24 h of collection.

*Hemolymph collection*

The third instars of *O. elegans* were rinsed three times with sterile distilled water to remove the soils and plant fibers. They were then surface sterilized with 75 % ethanol for a few seconds, and chilled on ice for 5–7 min. Two groups of 10 larvae each were separately injected in the dorsal blood vessel with 20 ng / 10 µL LPS from *E. coli* serotype O26:B6 (Sigma-Aldrich, St. Louis, MO, USA) using a Hamilton syringe (25-gauge needle) according to Mazza *et al*. (2011). Hemolymph of the first and second groups was obtained from the dorsal blood vessel of larvae 4 and 24 h post-injection, respectively. A sample of 1 ml of hemolymph was collected from each larva and placed in sterilized 2-ml Eppendorf® tubes (Sigma-Aldrich, St. Louis, MO, USA) containing an anticoagulant solution described by Mazza *et al*. (2011). A parallel control group included non-injected larvae. Each injected and non-injected group was replicated three times. The same procedures were also conducted 4 and 24 h post-injection with 50 µL of carboxylate-modified polystyrene latex beads with a diameter of 0.9 µm in a 10 % aqueous suspension (Sigma-Aldrich, St. Louis, MO, USA).

*Total hemocyte count, differential hemocyte count, and hemocyte morphology*

The total number of hemocytes was counted using a Neubauer hemocytometer (DHC-No 1) (ThermoFischer Scientific, Waltham Massachusetts, USA). The hemolymph that was obtained from *O. elegans* larvae 4 and 24 h post-injection with LPS was drawn into a Thoma white blood cell diluting pipette up to the 0.5 mark and then diluted 20 times with Toissin's solution as described by Perveen and Ahmad (2017). After discarding the first three drops, one drop was placed near the edge of a coverslip of a Neubauer ruling and counting chamber, and it was automatically filled by capillary action. Four white-cell squares from both the upper and lower chambers were counted. The total hemocyte count (THC) was calculated by using the formula suggested by Jones (1962). Hemocytes in a parallel control using hemolymph from non-injected larvae were also counted using the same approach. Each treatment was replicated three times. The differential hemocyte count (DHC) was calculated in terms of the percentage of each hemocyte type in the total cells counted (Jones, 1964), using an oil immersion phase-contrast microscope (OLYMPUS CX41, Hamburg, Germany) at 1000 × magnification.

For the examination of the hemocyte morphology, 100 µL of the hemolymph that was collected from *O. elegans* larvae 4 and 24 h post-injection with LPS was smeared on a sterilized glass slide, air-dried, and fixed for 2 min with absolute ethanol. Blood films were then stained with freshly prepared 4 % Giemsa stain (Sigma-Aldrich, St. Louis, MO, USA) for 15 min and subsequently washed with distilled water. The slide was air-dried and mounted in Canada Balsam (Sigma-Aldrich, St. Louis, MO, USA). The smears were examined using optical microscope (OLYMPUS BX51) with a digital camera (18-megapixel SC180, OLYMPUS) at 1000 × magnification. Hemolymph of non-injected larvae served as the control experiment. Each treatment was replicated three times.

In vivo *phagocytosis*

Hemolymph that was collected from *O. elegans* larvae 4 and 24 h post-injection with latex was centrifuged at 3000 *g* for 10 min at 4 °C to precipitate hemocytes. Then, the precipitated hemocytes were fixed in a 0.1 M cacodylate buffer with a pH of 7.2 with 2.5 % glutaraldehyde solution for 2 h. The fixed pellets were then post-fixed in cacodylate buffer with 1% osmium tetroxide solution for 2 h, dehydrated in a graded ethanol solution, and embedded in Araldite® (Sigma-Aldrich, St. Louis, MO, USA). The ultrathin sections, which were prepared using a Leica Ultracut R microtome (Leica Microsystems GMBH, Wetzlar, Germany), were stained with uranyl acetate and lead citrate. They were then examined using a JEM-2100F transmission electron microscope (JEOL, USA). A parallel control of ultrathin sections of hemocytes of non-injected larvae was also conducted.

*Bacterial strains and culture conditions*

To characterize antibacterial activity, three Gram-positive strains, *S. aureus* (ATCC 6538), *M. luteus* (ATCC 10240), and *B. subtilis* (ATCC 6051) and a Gram-negative strain, *E. coli* (ATCC 10536), were assayed. All strains were maintained at -20 °C in brain heart infusion broth with 20 % v/v glycerol. Before experimental use, each bacterial culture was propagated separately at 35 °C in a medium of 0.6 % bactopeptone, 0.4 % casein hydrolysate, 0.15 % beef extract, 0.3 % yeast extract, and 0.1 % glucose, pH 7.9 following Bíliková *et al*. (2001). Bacterial standard strains were purchased from the University Boulevard Manassas, VA 20110 USA.

*Agar well diffusion method*

Hemolymph that was collected from *O. elegans* larvae 4 h and 24 h post-injection with LPS was centrifuged at 3000 *g* for 10 min at 4 °C. The plasma supernatant was kept at -20 °C in Eppendorf tubes containing an anticoagulant solution following Mazza *et al*. (2011). Four serial dilutions of plasma, corresponding to 2, 1, 0.5, and 0.25 mg proteins/ml, were prepared with phosphate-buffered saline with a pH of 7.2. Each of the above-mentioned bacterial strains was inoculated into nutrient broth and incubated overnight at 37 °C until growth was 1.5 mg/ml at an optical density of 640 nm. Mueller-Hinton agar plates were prepared by dispensing 25 ml of a sterile Diagnostic Sensitivity Test Agar (Dehydrated, Thermo Scientific™ Oxoid™) into sterile Petri dishes with a diameter of 10 cm. A growth inhibition zone assay was conducted, according to Magaldi *et al*. (2004) and Valgas *et al*. (2007). The solidified agar plates were streaked uniformly with one of each of the above-mentioned cultured bacterial strains. Four equidistant wells, with a diameter of 5 mm, were made in the agar, and each well was filled with 50 µL of each dilution of plasma. The same procedures were applied to a parallel control using plasma of non-injected larvae. All plates were left for 1 h at room temperature for complete diffusion, after which they were incubated at 37 °C for 24 h. The diameters of the agar inhibition zones were measured in mm. Each assay was replicated three times. Total protein content in LPS-injected plasma and that of non-injected plasma was quantified according to the methods of Bradford *et al*. (1976).

*Statistical analysis*

All experiments were conducted according to a completely randomized design. Data were checked for normality prior to analysis using Shapiro-Wilk test and were symmetric. Data are presented as the mean ± standard error (SE) and were analyzed using Student's *t*-test between treatments and controls. Comparison between the two times of treatments (4 and 24 h) was also analyzed using Student's *t*-test. The significance level was set at $p \leq 0.05$, and all statistical analyses were conducted using IBM® SPSS® Statistics, version 25 (IBM® Corp. Armonk, NY, USA).

**Results**

*Total hemocyte count*

Injection of *O. elegans* larvae with LPS significantly increased the THC 4 h (36.74%; $t = 20.84$, $df = 4$, $p < 0.001$) and 24 h (33.23%; $t = 13.45$, $df = 4$, $p < 0.001$) post-injection compared to that of the control (Fig. 1). The THC of *O. elegans* larvae 24 h was not significantly different ($p > 0.05$) from that 4 h post-injection with LPS.

*Differential hemocyte count*

Phase-contrast light microscopy revealed that five hemocyte types were identified in *O. elegans* larvae: prohemocytes, granulocytes, plasmatocytes,

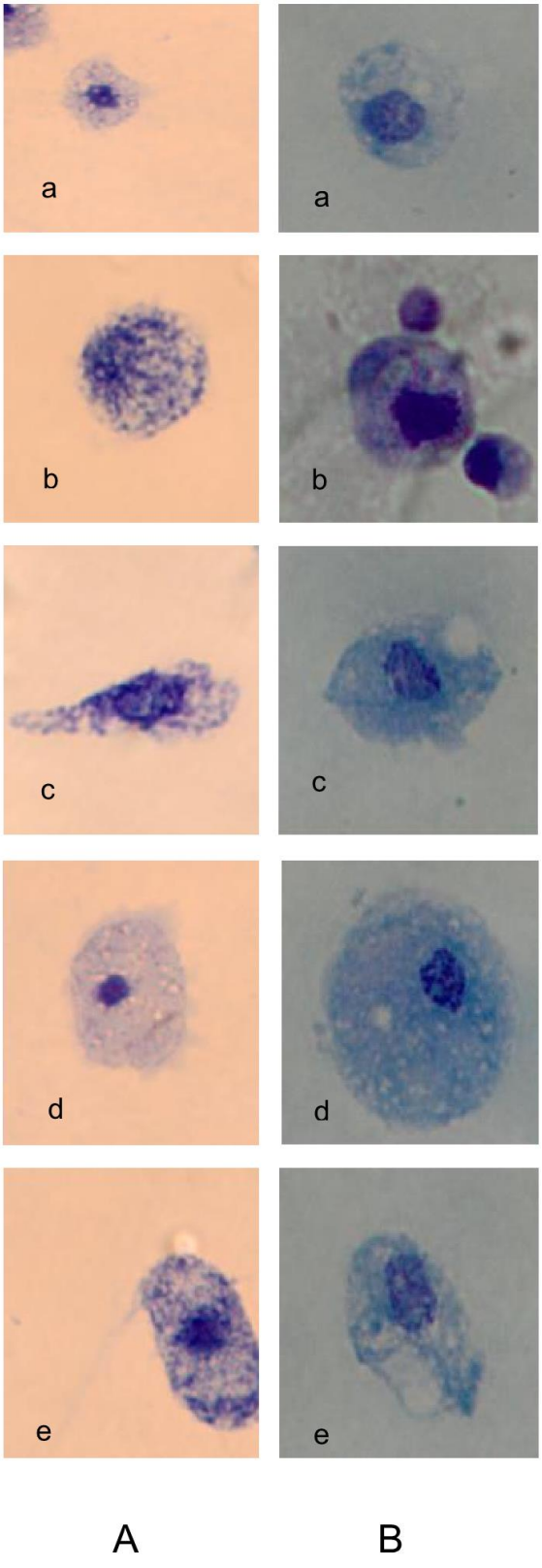


**Fig. 3** Light microscopic photomicrographs (1000 ×) of normal Giemsa-stained hemocytes of *O. elegans* third instars (column A), and 4 h post-injection with LPS (column B). a. Prohemocytes. b. Granulocytes. c. Plasmatocytes. d. Oenocytoids. e. Spherulocytes

oenocytoids, and spherulocytes. Four hours post-injection with LPS, the number of oenocytoids in the hemolymph of *O. elegans* larvae was significantly decreased ($df = 4$, $t = 5.47$, $p = 0.005$) compared to that of the control (Fig. 2A). After 24 h of exposure to LPS, the number of each hemocyte type did not change ($p > 0.05$) in the hemolymph of the *O. elegans* larvae compared to that of the controls (Fig. 2B). A variable change in the number of each hemocyte type 24 h compared to that 4 h post-injection with LPS was observed: the prohemocytes ($df = 4$, $t = 23.02$, $p < 0.001$) and oenocytoids ($df = 4$, $t = 25.58$, $p < 0.001$) were significantly increased. In contrast, the plasmatocytes were significantly decreased ($df = 4$, $t = 5.45$, $p = 0.005$).

*Hemocyte morphology*

A particular morphology was observed in each hemocyte type: the prohemocytes were round and small with a central nucleus and homogenous cytoplasm, the granulocytes were round and heavily granulated with a central nucleus, the plasmatocytes looked spindle-shaped and had pointed ends and fine poorly stained granules, the oenocytoids contained a round and eccentric nucleus and homogeneous cytoplasm, and the spherulocytes were oval with cytoplasm containing large, round vesicles or spherules (Figs 3A, 4A).

Four hours after the injection of *O. elegans* larvae with LPS, some changes were observed in hemocyte morphology compared to those of the controls: the central nucleus of the prohemocytes occupied most of the cytoplasm (Fig. 3B-a), and the nucleus of the granulocytes was darkly-stained (Fig. 3B-b). After 24 h of exposure to LPS, the cytoplasm in the prohemocytes formed a thin layer around the nucleus (Fig. 4B-a), while the cytoplasm of the granulocytes was highly degranulated, and the nucleus was more central when compared to the control (Fig. 4B-b). In addition, the plasmatocytes were swollen with degranulated cytoplasm (Fig 4B-c), the cytoplasm of the oenocytoids appeared transparent (Fig. 4B-d), and the spherulocytes contained dense spherules (Fig. 4B-e).

In vivo *phagocytosis*

Transmission electron microscopy (TEM) revealed that granulocytes and plasmatocytes were the phagocytic cells in *O. elegans* larvae. These granulocytes were round with many granules and a central nucleus (Figs 5A-a, 6A-a), and the plasmatocytes were spindle-shaped with a large and round nucleus (Figs 5A-b, 6A-b).

Four hours post-injection with latex beads, the granulocytes and plasmatocytes showed conspicuous phagocytic activity that was more pronounced in granulocytes: several phagosomes containing latex beads were observed. The granules fused with the phagosomes and discharged their contents inside them, making the space around the latex beads more electron-dense. Multi-vesicular bodies were also present (Fig. 5B-a). The phagocytic granulocytes showed degranulated cytoplasm filled with latex beads (Fig. 5B-b), and the phagocytic plasmatocytes, which contained latex bead particles inside their phagosomes (Fig. 5B-c), were irregular in shape, varying from round to very

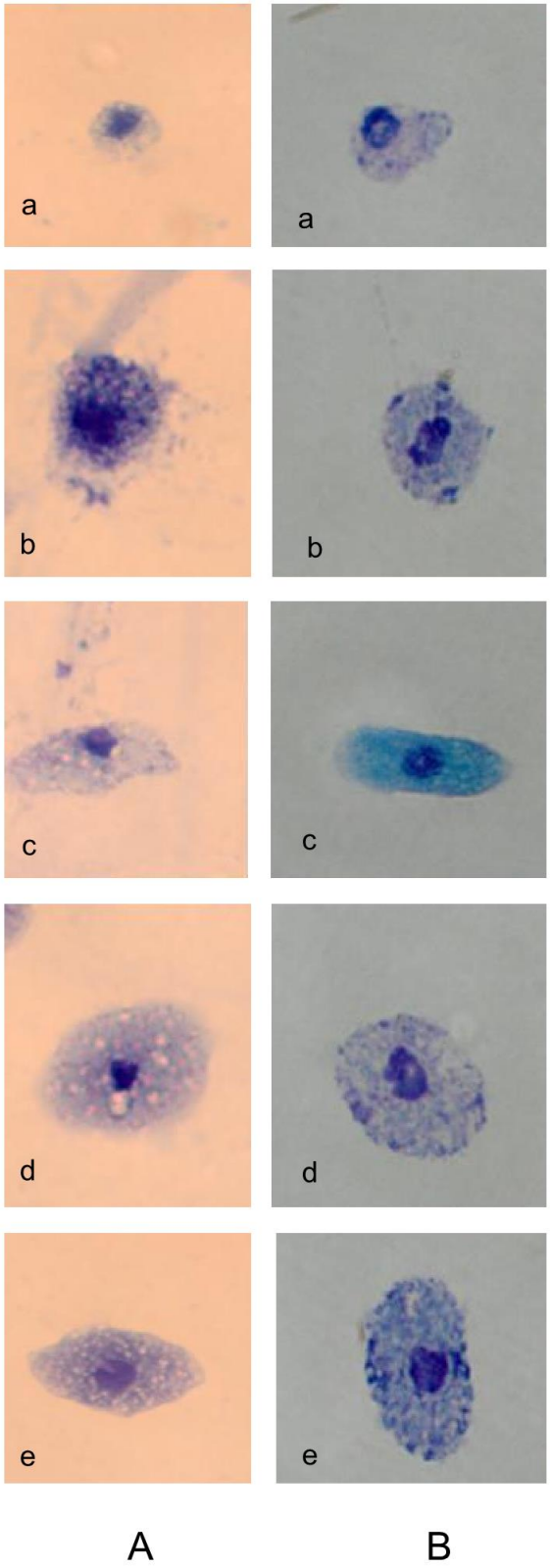


**Fig. 4** Light microscopic photomicrographs (1000 ×) of normal Giemsa-stained hemocytes of *O. elegans* third instars (column A), and 24 h post-injection with LPS (column B). a. Prohemocytes. b. Granulocytes. c. Plasmatocytes. d. Oenocytoids. e. Spherulocytes

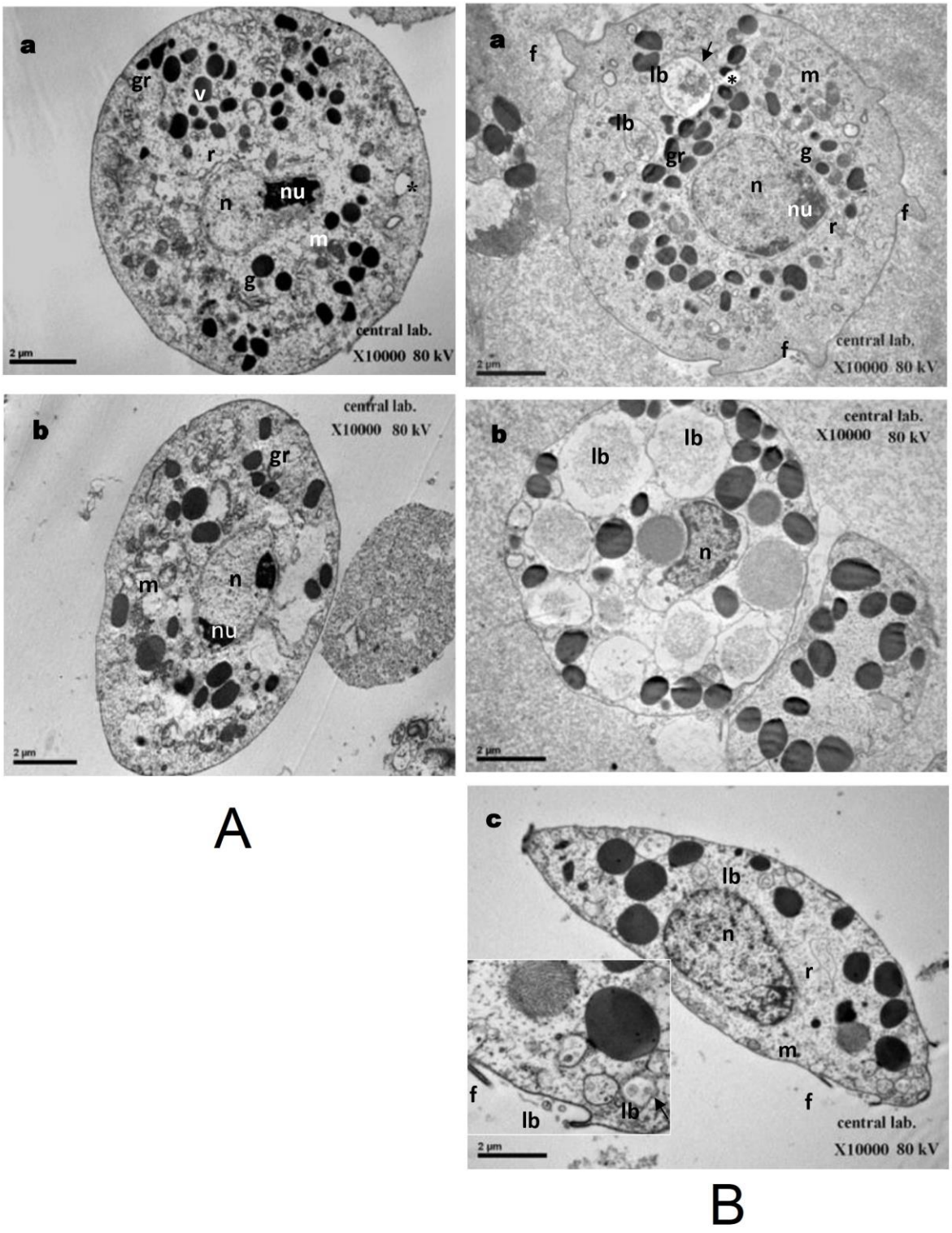


**Fig. 5** A. Transmission electron microscopy photomicrographs of normal hemocytes of *O. elegans* third instars 4 h without injection with latex beads. a. Granulocyte with many typical granules (*gr*), lobated nucleus (*n*) with an evident nucleolus (*nu*), rough endoplasmic reticulum (*r*), mitochondria (*m*), Golgi complex (*g*), round vesicles (*asterisks*), and electron-dense vesicles (*v*). b. Oval-shaped plasmatocyte with few granules (*gr*), nucleus (*n*) with evident nucleolus (*nu*), and mitochondria (*m*). Scale bar = 2 µm. B. Transmission electron microscopy photomicrographs of hemocytes of *O. elegans* third instars 4 h post-injection with latex beads. a. Granulocyte showing several phagosomes with latex beads (*lb*), a nucleus (*n*) with an evident nucleolus (*nu*), rough endoplasmic reticulum (*r*), cytoplasm showing Golgi complex (*g*), many filopodia (*f*), mitochondria (*m*), and round vesicles (*asterisks*). b. Degranulated granulocyte with many vacuoles containing latex beads (*lb*). c. Spindle-shaped plasmatocyte with many phagosomes containing latex beads (*lb*), a heterochromatic nucleus (*n*), rough endoplasmic reticulum (*r*), mitochondria (*m*), and filopodia (*f*) engulfing latex beads (*lb*) (inset). Scale bar = 2 µm

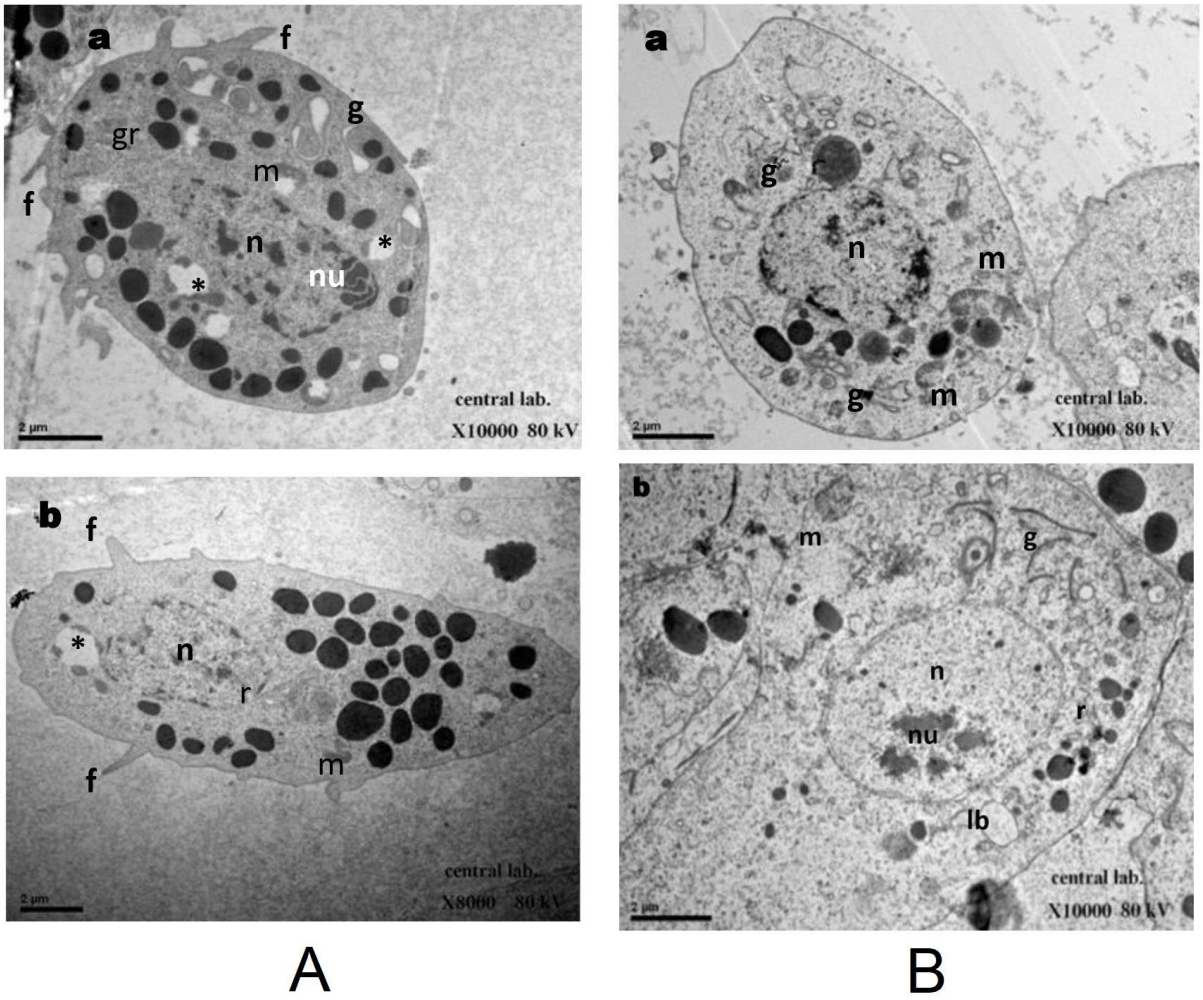


**Fig. 6** A. Transmission electron microscopy photomicrographs of normal hemocytes of *O. elegans* third instars 24 h without injection with latex beads. a. Granulocyte with granules (*gr*), indented nucleus (*n*) with nucleolus (*nu*), Golgi complex (*g*), filopodia (*f*), mitochondria (*m*), and round vesicles (*asterisks*). b. Spindle-shaped plasmatocyte with filopodia (*f*), nucleus (*n*), mitochondria (*m*), and rough endoplasmic reticulum (*r*). Scale bar = 2 µm. B. Transmission electron microscopy photomicrographs of hemocytes of *O. elegans* third instars 24 h post-injection with latex beads. a. Degranulated granulocyte, nucleus (*n*), mitochondria (*m*), and Golgi complex (*g*). b. Plasmatocyte showing many elongated Golgi complex (g), an eccentric nucleus (*n*) with nucleolus (*nu*), mitochondria (*m*), rough endoplasmic reticulum (*r*), and phagosomes with latex beads (*lb*). Scale bar = 2 µm

elongated, with deeply indented and heterochromatic nuclei. After 24 h of exposure to latex, the granulocytes became highly degranulated (Fig. 6B-a), and the plasmatocytes exhibited an eccentric nucleus, many elongated Golgi complexes and phagosomes containing latex beads (Figs 6B-b).

*Antibacterial activity*

Four hours post-injection with LPS, the diameters of the agar inhibition zones of *S. aureus* were significantly lower than those of the controls (non-injected) at the four tested concentrations of total plasma proteins ($df$ = 4, $t$ = 4.70, $p$ = 0.009; $df$ = 4, $t$ = 4.43, $p$ = 0.011; $df$ = 4, $t$ = 10.35, $p$ = 0.001; $df$ = 4, $t$ = 10.98, $p$ < 0.001 for 2, 1, 0.5, and 0.25 mg protein/ml, respectively) (Fig. 7A), indicating the suppression of antibacterial activity. However, after 24 h of exposure to LPS, the agar inhibition zone diameters of *S. aureus* were significantly larger than those of the controls at 0.25 mg protein/ml ($df$ = 4, $t$ = 15.01, $p$ < 0.001) (Fig. 7B), suggesting antibacterial activity. The agar inhibition zone diameters of S. *aureus* were significantly increased 24 h compared to those 4 h post-injection with LPS at 2 mg protein/ml ($df$ = 4, $t$ = 2.68, $p$ = 0.05), 0.5 mg/ml ($df$ = 4, $t$ = 4.10, $p$ = 0.015) and 0.25 mg/ml ($df$ = 4, $t$ = 7.65, $p$ = 0.002).

The plasma proteins of LPS-injected *O. elegans* larvae resulted in a significant increase in the diameters of the agar inhibition zones of *M. luteus* 4 h post-injection at the four tested concentrations of

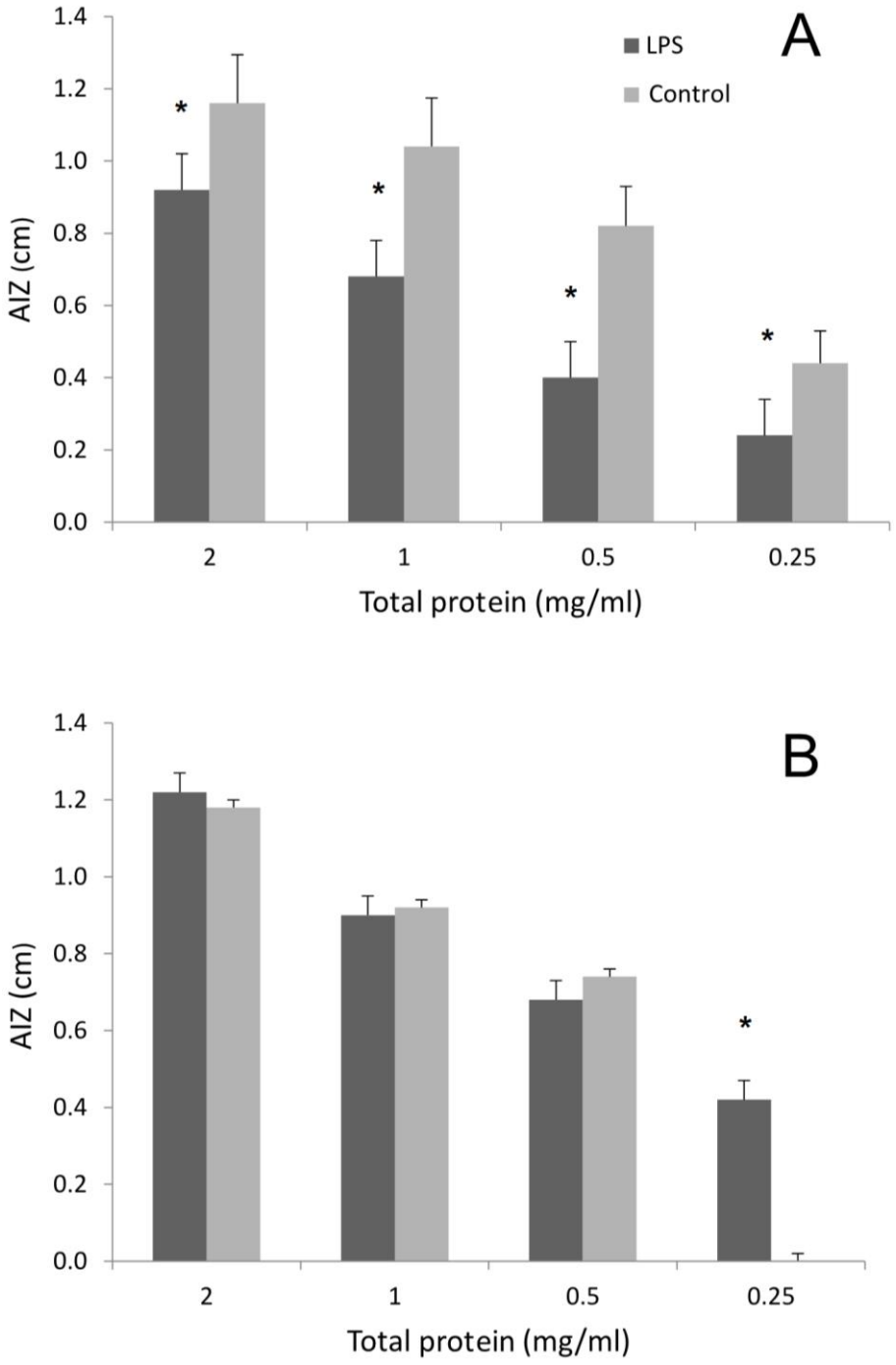


**Fig. 7** Agar inhibition zone (AIZ) diameters of *S. aureus* growth 4 h (A), and 24 h post-injection (B) of *O. elegans* third instars with lipopolysaccharide (LPS). Data are presented as the mean ± SE. *, Significant at $p < 0.05$ compared to the control, using Student's *t*-test

plasma proteins compared to those of the controls ($df = 4$, $t = 2.06$, $p = 0.019$; $df = 4$, $t = 4.74$, $p = 0.009$; $df = 4$, $t = 5.0$, $p = 0.008$; $df = 4$, $t = 4.81$, $p = 0.009$ for 2, 1, 0.5, and 0.25 mg protein/ml, respectively) (Fig. 8A). Whereas, after 24 h of exposure to LPS, the diameters of the agar inhibition zones of *M. luteus* were significantly decreased compared to those of the controls at 0.5 mg protein/ml ($df = 4$, $t = 4.36$, $p = 0.012$) and 0.25 mg protein/ml ($df = 4$, $t = 13.19$, $p < 0.001$) (Fig. 8B). The agar inhibition zone diameters of *M. luteus* were significantly decreased 24 h compared to those 4 h post-injection with LPS at 1 mg/ml ($df = 4$, $t = 5.08$, $p = 0.007$), 0.5 mg/ml ($df = 4$, $t = 8.60$, $p = 0.001$) and 0.25 mg/ml ($df = 4$, $t = 10.25$, $p = 0.001$).

The agar inhibition zone diameters of *B. subtilis* were significantly increased compared to those of the controls 4 h post-injection with LPS at the four

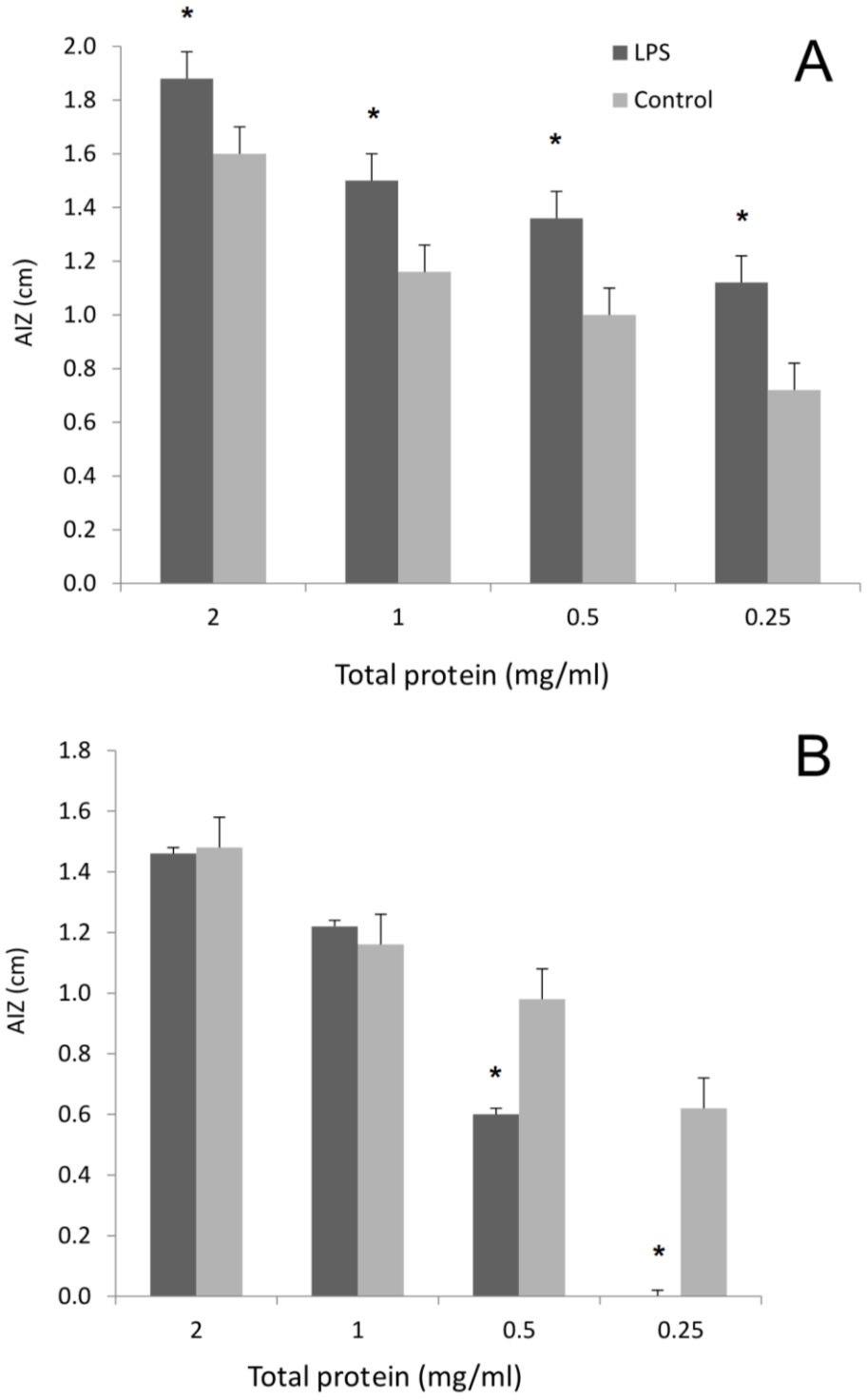


**Fig. 8** Agar inhibition zone (AIZ) diameters of *M. luteus* growth 4 h (A), and 24 h post-injection (B) of *O. elegans* third instars with lipopolysaccharide (LPS). Data are presented as the mean ± SE. *, Significant at $p < 0.05$ compared to the control, using Student's *t*-test

tested concentrations of plasma proteins ($df = 4$, $t = 2.50$, $p = 0.05$; $df = 4$, $t = 2.71$, $p = 0.05$; $df = 4$, $t = 5.29$, $p = 0.006$; $df = 4$, $t = 11.69$, $p < 0.001$ for 2, 1, 0.5, and 0.25 mg protein/ml, respectively) (Fig. 9A), indicating antibacterial activity. In contrast, the agar inhibition zone diameters of *B. subtilis* were significantly decreased compared to those of the controls after 24 h of injection with LPS at all the concentrations of plasma proteins tested, indicating the suppression of antibacterial activity ($df = 4$, $t = 11.26$, $p < 0.001$; $df = 4$, $t = 76.70$, $p < 0.001$; $df = 4$, $t = 12.70$, $p < 0.001$; $df = 4$, $t = 10.04$, $p = 0.001$ for 2, 1, 0.5, and 0.25 mg

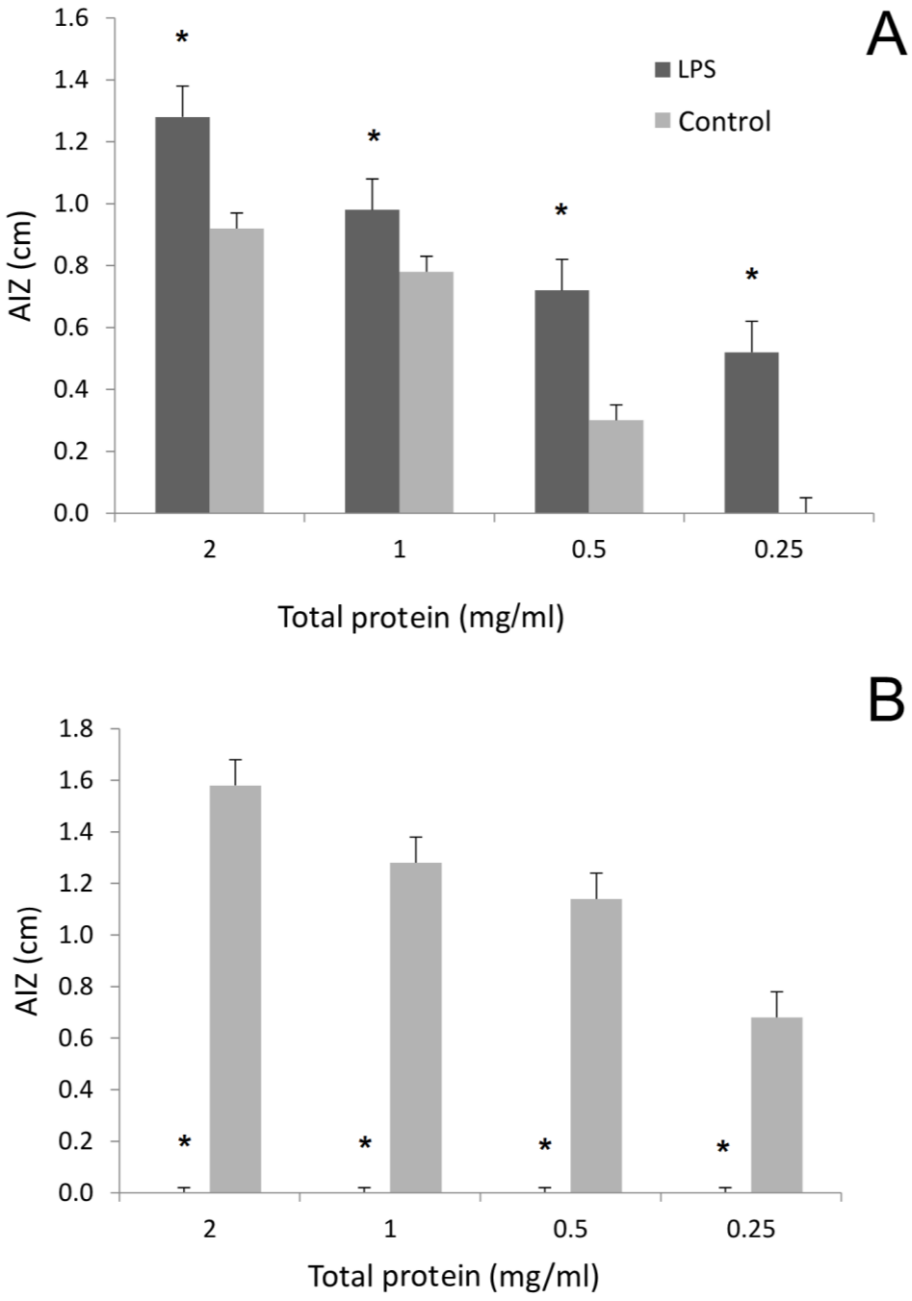


**Fig. 9** Agar inhibition zone (AIZ) diameters of *B. subtilis* growth 4 h (A), and 24 h post-injection (B) of *O. elegans* third instars with lipopolysaccharide (LPS). Data are presented as the mean ± SE. *, Significant at $p < 0.05$ compared to the control, using Student's *t*-test

mg protein/ml, respectively) (Fig. 9B). The agar inhibition zone diameters of *B. subtilis* were significantly decreased 24 h compared to those 4 h post-injection with LPS at the four concentrations of plasma protein tested ($df = 4$, $t = 10.25$, $p = 0.001$; $df = 4$, $t = 11.11$, $p < 0.001$; $df = 4$, $t = 11.90$, $p < 0.001$; $df = 4$, $t = 11.41$, $p < 0.001$ for 2, 1, 0.5 and 0.25 mg protein/ml, respectively).

The diameters of the agar inhibition zones of *E. coli* were significantly smaller than those of the controls 4 h post-injection of *O. elegans* larvae with LPS at 2 mg protein/ml ($df = 4$, $t = 7.89$, $p = 0.001$), 0.5 mg protein/ml ($df = 4$, $t = 6.63$, $p = 0.003$), and 0.25 mg protein/ml ($df = 4$, $t = 5.81$, $p = 0.004$) (Fig. 10A). After 24 h of exposure to LPS, the agar inhibition zone diameters of *E. coli* were significantly smaller than those of the controls at 2 mg protein/ml ($df = 4$, $t = 7.37$, $p = 0.002$), 1 mg protein/ml ($df = 4$, $t = 13.25$, $p < 0.001$), and 0.5 mg protein/ml ($df = 4$, $t = 17.70$, $p < 0.001$), whereas at 0.25 mg protein/ml the diameters of the agar inhibition zones of *E. coli* were significantly larger than those of the controls

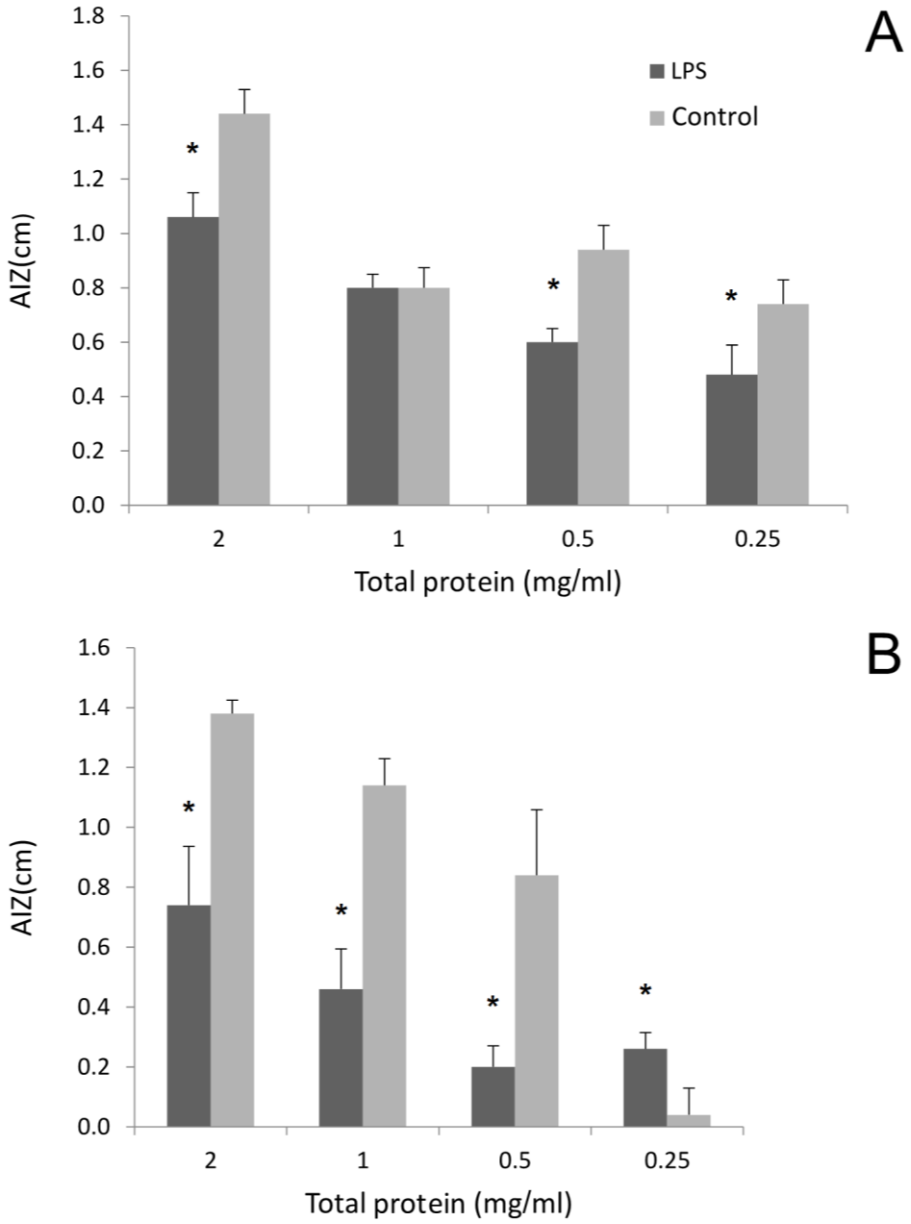


**Fig. 10** Agar inhibition zone (AIZ) diameters of *E. coli* growth 4 h (A), and 24 h post-injection (B) of *O. elegans* third instars with lipopolysaccharide (LPS). Data are presented as the mean ± SE. *, Significant at $p < 0.05$ compared to the control, using Student's *t*-test

(*df = 4, t* = 12.98, $p < 0.001$) (Fig. 10B), indicating antibacterial activity. The agar inhibition zone diameters of *E. coli* were significantly decreased 24 h compared to those 4 h post-injection with LPS at the four concentrations of plasma protein tested (*df* = 4, *t* = 9.15, $p < 0.001$; *df* = 4, *t* = 10.55, $p < 0.001$; *df* = 4, *t* = 14.36, $p < 0.001$; *df* = 4, *t* = 4.05, $p = 0.016$ for 2, 1, 0.5 and 0.25 mg protein/ml, respectively).

**Discussion**

The present study represents the first report on the inducible immune response of *O. elegans*. The immune response of this insect was time post-treatment dependent. Although the THC 24 h post-injection with LPS was not significantly affected compared to that 4 h post-injection, the THC was significantly increased compared to the controls at each time treatment. Patton (1961) implicated the hemocytes of insects in the detoxification of toxic xenobiotics. The number of prohemocytes and oenocytoids were significantly increased with the increase of time post-injection with LPS from 4 h to 24 h. The prohemocytes are the progenitor stem cells that can differentiate into other hemocyte types for phagocytosis to combat biotic and abiotic foreign invaders or apoptotic bodies (Hernandez *et al.*,

1999; De Silva *et al.*, 2000; Yamashita and Iwabuchi, 2001; Lavine and Strand, 2002). Dorrah *et al*. (2019) suggested that increased oenocytoids in the fleshfly, *Sarcophaga argyrostoma* (Robineau-Desvoidy) (Diptera: Sarcophagidae) last instars 36 h post-treatment with the limonoid, azadirachtin, may have been an attempt by larvae to compensate the decrease in phenoloxidase (PO) activity in the hemocytes of treated larvae.

Hemocyte morphology and phagocytosis in *O. elegans* larvae were also time dependent, with the greatest effect 24 h post-injection with LPS and latex, respectively.

A declining trend in antibacterial activity, 24 h after exposure to LPS, was observed for the Gram-positive bacteria studied, except for *S. aureus* where the antibacterial activity was increased 24 h compared to that 4 h post-injection with LPS. This finding suggests that the humoral immune system of *O. elegans* cannot recognize *S. aureus* 4 h post-exposure to LPS. Nevertheless, this hypothesis needs future confirmatory experiments.

Four hours post-injection of *O. elegans* larvae with LPS, the number of oenocytoids was significantly decreased compared to the control. The decrease in the number of oenocytoids suggests the immunosuppressive effect of LPS, where these cells are known to release the precursor of PO (prophenoloxidase, proPO), which plays a role in the melanization of the hemolymph (Ribeiro *et al*., 1996).

The insect hemogram and the peculiar hemocyte combination in each developmental stage are important and serve as indicators of environmental adaptability (Sharma *et al*., 2008). Hemocytes, *via* a change in cell number, are frequently used to demonstrate the cytogenetic damage induced by toxic xenobiotics (Wessel *et al*., 2007).

Our study identified five hemocyte types in *O. elegans* larvae: prohemocytes, granulocytes, plasmatocytes, oenocytoids, and spherulocytes. Likewise, the same hemocyte types have been reported in *R. ferrugineus* larvae (Manachini *et al*., 2011). The finding that granulocytes and plasmatocytes were the most abundant hemocytes in *O. elegans* agrees with results reported by Manachini *et al*. (2011) and Kwon *et al*. (2014).

TEM observations revealed that granulocytes and plasmatocytes were the phagocytic hematocytes in the hemolymph of *O. elegans* larvae. The higher phagocytic activity of granulocytes suggests that they were the primary phagocytes, and the phagocytic activity of granulocytes and plasmatocytes may explain their substantial proportion in *O. elegans* larvae. This is in line with findings for other insects on the involvement of granulocytes and plasmatocytes in phagocytosis (Manachini *et al*., 2011; Kwon *et al*., 2014; Zhang and Zhang, 2019). Our findings of ultrastructural changes in granulocytes and plasmatocytes due to phagocytosis are also comparable to those reported for most insects (Giulianini *et al*., 2003; Lemaitre and Hoffmann, 2007; Borges *et al*., 2008; Amaral *et a*l., 2010; Kwon *et al*., 2014; Zhang and Zhang, 2019). In addition, several studies have reported that phagocytosis of latex beads in insects has been regulated by signaling pathways that could be initiated from the phagosome including activation of the nuclear factor κB (NF-κB) and activation of mitogen-activated protein kinases (MAPK) (Fratti *et al*., 2001; Lamprou *et al*., 2007) and involves both the zipper and trigger mechanisms (Borges *et al*., 2008). Phagocytosis of latex beads do not depend on proPO activation (Mavrouli *et al*., 2005; Lamprou et al., 2007). Phagocytosed macromolecules have also been broken down by hydrolase localized in the lysosomes of insect hemocytes (Callewaert and Michiels, 2010; Wu and Yi, 2015).

The agar well diffusion method demonstrated that plasma proteins of *O. elegans* larvae in our study showed antibacterial activity against the bacterial strains studied. In agreement with our results, the antibacterial activity of hemolymph of *R. ferrugineus* and the coconut palm rhinoceros beetle, *Oryctes rhinoceros* (L.) (Coleoptera: Scarabaeidae), against the same tested bacteria has also been reported (Mazza *et al*., 2011; Rabeeth *et al*., 2012; Mastore *et al*., 2015). Most AMPs exert their antibacterial effects by interacting with and destabilizing both plasma membrane and bacterial walls, eventually leading to cell death, and some AMPs can enter the cell and interact with cytoplasmic factors (Ding *et al*., 2003; Brogden, 2005; Alves *et al*., 2010; Mastore *et a*l., 2015). Evidence in the literature suggests that host AMPs could act in cooperation with other immunocompetent factors to modulate innate immune responses (Hoffman and Reichhart, 2002).

Overall, the three tested Gram-positive bacteria, *S. aureus*, *M. luteus*, and *B. subtilis*, were more sensitive than the Gram-negative bacterium, *E. coli*. This sensitivity may be attributed to the fact that Gram-positive bacteria are monoderms and have a single lipid layer, whereas Gram-negative bacteria are diderms and have two layers. The presence of the outer cell membrane in Gram-negative bacteria is thought to play an important role as a protective mechanism against antimicrobial agents and antibiotic selection pressure (Sewify *et al*., 2017). Furthermore, some species of Gram-negative bacteria, such as *Klebsiella* spp., are encapsulated in prominent polysaccharide capsules that provide them more resistance and protection against antibiotics (Podschun and Ullmann, 1998).

Insects recognize PAMPs (e.g. LPS) as a result of the interaction with endogenous pattern recognition receptors (PRRs). The interaction of PAMPs and PRRs elicits humoral and cellular defence, leading to the elimination of foreign pathogens (Hoffmann *et al*., 1999; Govind, 2008). The presence of microorganisms and their PAMPs inside insects' hemocoelic cavity triggers various short-term immune processes, such as proPO-PO system activation (humoral encapsulation) or phagocytosis (Mastore *et al*. 2015). However, these defence processes are only successful in the presence of a limited infection; when bacterial proliferation overcomes short-term defence, the onset of antibacterial responses, performed by AMPs and lysozymes, are the most effective

mechanism to prevent host septicemia (Yeaman and Yount, 2003).

In conclusion, our results point to the importance of understanding the inducible immune response of *O. elegans*. This may open new perspectives for the biological control of this insect. Furthermore, *O. elegans* could represent a kind of "*living laboratory*" in which to identify new compounds with antibacterial activity that might be useful for the development of innovative drugs of natural origin, which are able to counteract the antibiotic resistance that currently presents a serious threat to human and animal health.

**Conflict of Interest**

On behalf of all authors, the corresponding author states that there is no conflict of interest.

**References**


Al-Ayedh HY, Al Dhafer HM. Does *Oryctes elegans* (Coleoptera: Scarabaeidae) abundance determine future abundance of *Rhynchophorus ferrugineus* (Coleoptera: Rhynchophoridae) in the date palms of Saudi Arabia? Afr. Entomol. 23: 43-47, 2015.

Alves CS, Melo MN, Franquelim HG, Ferre R, Planas M, Feliu L, *et al*. *Escherichia coli* cell surface perturbation and disruption induced by antimicrobial peptides BP100 and pepR. J. Biol. Chem. 285: 27536-27544, 2010.

Amaral IM, Moreira Neto JF, Pereira GB, Franco MB, Beletti ME, Kerr WE, *et al.* Circulating hemocytes from larvae of *Melipona scutellaris* (Hymenoptera, Apidae, Meliponini): cell types and their role in phagocytosis. Micron 41: 123-129, 2010.

Atwa AA. Biological control potential of two steinernematid species against the date fruit stalk borer (*Oryctes elegans* Prell, Coleoptera: Scarabaeidae). J. Insect Sci. 18(3): 26; 1-8, 2018.

Bedford GO, Al-Deeb MA, Khalaf MZ, Mohammadpour K, Soltani R. Dynastid beetle pests. In: Wakil W, Faleiro JR, Mille TA (eds), Sustainable pest management in date palm: current status and emerging challenges, sustainability in plant and crop protection, Springer, Springer Nature, Cham, Switzerland, pp 73-108, 2015.

Bíliková K, Wu GS, Šimúth J. Isolation of a peptide fraction from honeybee royal jelly as a potential antifoulbrood factor. Apidologie 32: 275-283, 2001.

Bogdan C, Rollinghoff M, Diefenbach A. Reactive oxygen and reactive nitrogen intermediates in innate and specific immunity. Curr. Opin. Immunol. 12: 64-76, 2000.

Borges AR, Santos PN, Furtado AF, Figueiredo FCBQ. Phagocytosis of latex beads and bacteria by hemocytes of the triatomine bug *Rhodnius prolixus* (Hemiptera: Reduvidae). Micron 39: 486-494, 2008.

Bradford MM. A rapid and sensitive method for the quantitation of microgram quantities of protein utilizing the principle of protein-dye binding. Anal. Biochem. 72: 248-254, 1976.

Brivio MF, Moro M, Mastore M. Down-regulation of antibacterial peptide synthesis in an insect model induced by the body-surface of an entomoparasite (*Steinernema feltiae*). Dev. Comp. Immunol. 30: 627-638, 2006.

Brogden KA. Antimicrobial peptides: pore formers or metabolic inhibitors in bacteria? Nature Rev. Microbiol. 3: 238-250, 2005.

Browne N, Heelan M, Kavanagh K. An analysis of the structural and functional similarities of insect hemocytes and mammalian phagocytes. Virulence 4: 597-603, 2013.

Bulet P, Stocklin R. Insect antimicrobial peptides: Structures, properties and gene regulation. Protein Peptide Lett. 12: 3-11, 2005.

Callewaert L, Michiels CW. Lysozymes in the animal kingdom. J. Biosci. 35: 127-160, 2010.

Cociancich S, Bulet P, Hetru, Hoffmann JA. The inducible antibacterial peptides of insects. Parasitol. Today 4: 132-139, 1994.

De Silva C, Dunphy GB, Rau ME. Interaction of haemocytes and prophenoloxidase system of fifth instar nymphs of *Acheta domesticus* with bacteria. Dev. Comp. Immunol. 24: 367-379, 2000.

Ding L, Yang L, Weiss TM, Waring AJ, Lehrer RI, Huang HW. Interaction of antimicrobial peptides with lipopolysaccharides. Biochemistry 42: 12251-12259, 2003.

Dorrah MA, Mohamed AA, Shaurub EH. Immunosuppressive effects of the limonoid azadirachtin, insights on a nongenotoxic stress botanical, in flesh flies. Pestic. Biochem. Physiol. 153: 55-66, 2019.

Engström YI. Insect immune gene regulation. In: Brey P, Hultmark D (eds), Molecular mechanisms of immune responses in insects, Chapman & Hall, London, UK, pp 211-244, 1998.

Fratti RA, Backer JM, Gruenberg J, Corvera S, Deretic V. Role of phosphatidylinositol 3-kinase and Rab5 effectors in phagosomal biogenesis and mycobacterial phagosome maturation arrest. J. Cell Biol. 154: 631-644, 2001.

Gálvez D, Chapuisat M. Immune priming and pathogen resistance in ant queens. Ecol. Evol. 4: 1761-1767, 2014.

Gillespie JP, Kanost MR, Trenczek T. Biological mediators of insect immunity. Annu. Rev. Entomol. 42: 611-643, 1997.

Giulianini PG, Bertolo F, Battistella S, Amirante GA. Ultrastructure of the hemocytes of *Cetonischema aeruginosa* larvae (Coleoptera, Scarabaeidae): involvement of both granulocytes and oenocytoids in *in vivo* phagocytosis. Tissue Cell 35: 243-251, 2003.

Govind S. Innate immunity in *Drosophila*: Pathogens and pathways. Insect Sci. 15: 29-43, 2008.

Hall CL, Wadsworth NK, Howard DR, Jennings EM, Farrell LD, Magnuson TS *et al*. Inhibition of microorganisms on a carrion breeding resource: the antimicrobial peptide activity of burying beetle (Coleoptera: Silphidae) oral and anal secretions. Environ. Entomol. 40: 669-678, 2011.

Hernandez S, Lanz H, Rodriguez MH, Torres JA, Martínez PA, Tsutsumi V. Morphological and

cytochemical characterization of female *Anopheles albimanus* (Diptera: Culicidae) haemocytes. J. Med. Entomol. 36: 426-434, 1999.

Hillyer JF. Insect immunology and hematopoiesis. Dev. Comp. Immunol. 58: 102-118, 2016.

Hillyer JF, Strand MR. Mosquito hemocyte-mediated immune responses. Curr. Opin. Insect Sci. 3: 14-21, 2014.

Hoffmann, JA. Innate immunity of insects. Curr. Opin. Immunol. 7: 4-10, 1995.

Hoffmann JA. The immune response of *Drosophila*. Nature 426: 33-38, 2003.

Hoffmann JA, Kafatos FC, Janeway CA Jr, Ezekowitz RAB. Phylogenetic perspectives in innate immunity. Science 284: 1313-1318, 1999.

Hoffmann JA, Reichhart JM. *Drosophila* innate immunity: an evolutionary perspective. Nat. Immunol. 3: 121-126, 2002.

Hull R, Katete R, Ntwasa M. Therapeutic potential of antimicrobial peptides from insects. Biotechnol. Mol. Biol. Rev. 7: 31-47, 2012.

Jones J.C. Current concepts concerning insect haemocytes. Am. Zool. 2: 209-246, 1962.

Jones J.C. Differential hemocyte counts from unfixed last stage *Galleria mellonella*. Am. Zool. 4: 337-346, 1964.

Kwon H, Bang K, Cho S. Characterization of the hemocytes in larvae of *Protaetia brevitarsis seulensis*: involvement of granulocyte-mediated phagocytosis. PLoS ONE 9 (8): e103620, 1-12, 2014.

Lamprou I, Mamali I, Dallas K, Fertakis V, Lampropoulou M, Marmaras VJ. Distinct signalling pathways promote phagocytosis of bacteria, latex beads and lipopolysaccharide in medfly haemocytes. Immunology 121: 314-327, 2007.

Latifian M, Rad B. Pathogenicity of the entomopathogenic fungi *Beauveria bassiana* (Balsamo) Vuillmin, *Beauveria brongniartii* Saccardo and *Metarhizium anisopliae* Metsch to adult *Oryctes elegans* Prell and effects on feeding and fecundity. Int. J. Agri. Crop Sci. 4: 1026-1032, 2012.

Lavine MD, Strand MR. Insect hemocytes and their role in immunity. Insect Biochem. Mol. Biol. 32: 1295-309, 2002.

Lemaitre B, Hoffmann JA. The host defense of *Drosophila melanogaster*. Annu. Rev. Immunol. 25: 697-743, 2007.

Magaldi S, Mata-Essayag S, Hartung de Capriles C, Perez C, Colella MT, Olaizola C, *et al*. Well diffusion for antifungal susceptibility testing. Int. J. Infect. Dis. 8: 39-45, 2004.

Manachini B, Arizza V, Parrinello D, Parrinello N. Hemocytes of *Rhynchophorus ferrugineus* (Olivier) (Coleoptera: Curculionidae) and their response to *Saccharomyces cerevisiae* and *Bacillus thuringiensis*. J. Invertebr. Pathol. 106: 360-365, 2011.

Mavrouli MD, Tsakas S, Theodorou GL, Lampropoulou M, Marmaras VJ. MAP kinases mediate phagocytosis and melanization via prophenoloxidase activation in medfly hemocytes. Biochim. Biophys. Acta 1744: 145-156, 2005.

Mastore M, Rossetti SB, Giovannardi S, Scarì G, Brivio MF. Inducible factors with antimicrobial activity after immune challenge in the haemolymph of red palm weevil (Insecta). Innate Immun. 21: 392-405, 2015.

Mazza G, Arizza V, Baracchi D, Barzanti GP, Benvenuti C, Francardi V, *et al*. Antimicrobial activity of the red palm weevil *Rhynchophorus ferrugineus.* Bull. Insectology 64: 33-41, 2011.

Nakatogawa S, Oda Y, Kamiya M, Kamijima T, Aizawa T, Clark KD, *et al*. A novel peptide mediates aggregation and migration of hemocytes from an insect. Curr. Biol. 19: 779-785, 2009.

Nappi AJ, Vass E. Cytotoxic reactions associated with insect immunity. Adv. Exp. Med. Biol. 484: 329-348, 2001.

Ntwasa M, Goto A, Kurata S. Coleopteran antimicrobial peptides: prospects for clinical applications. Int. J. Microbiol. 2012: 1-8, 2012.

Patton RL. The detoxification function of insect haemocytes. Ann. Entomol. Soc. Am. 54: 696-698, 1961.

Perveen N, Ahmad M. Toxicity of some insecticides to the haemocytes of giant honeybee, *Apis dorsata* F. under laboratory conditions. Saudi J. Biol. Sci. 24: 1016-1022, 2017.

Podschun R, Ullmann U. *Klebsiella* spp. as nosocomial pathogens: epidemiology, taxonomy, typing methods, and pathogenicity factors. Clin. Microbiol. Rev. 11: 589-603, 1998.

Pradipta AP, Wagiman FX, Witjaksono. The potency of collecting larvae of *Oryctes rhinoceros* L. (Coleoptera: Scarabaeidae) in the oil palm plantation. AGRIVITA J. Agric. Sci. 42: 153-159, 2020.

Rabeeth M, Muthukumar M, Balaji Rajkumar M, Kesava Kumar H. Isolation, evaluation and purification of antibacterial peptides from rhinoceros beetle, *Oryctes rhinoceros* (L.). GERF Bull. Biosci. 3: 16-22, 2012.

Ribeiro C, Simoes N, Brehelin M. Insect immunity: the haemocytes of the armyworm *Mythimna unipuncta* (Lepidoptera: Noctuidae) and their role in defence reactions. *in vivo* and *in vitro* studies. J. Insect Physiol. 42: 815-822, 1996.

Sewify GH, Hamada HM, Alhadrami HA. *In vitro* evaluation of antimicrobial activity of alimentary canal extracts from the red palm weevil, *Rhynchophorus ferrugineus* Olivier larvae. BioMed. Res. Int. 2017: 1-6, 2017.

Sharma PR, Sharma OP, Saxena BP. Effect of sweet flag rhizome oil (*Acorus clamus*) on haemogram and ultrastructure of haemocytes of the tobacco armyworm, *Spodoptera litura* (Lepidoptera; Noctuidae). Micron 39: 544-551, 2008.

Shaurub EH. Immunomodulation in insects post-treatment with abiotic agents: A review. Eur. J. Entomol. 109: 303-316, 2012.

Sheehan G, Farrell G, Kavanagh K. Immune priming: the secret weapon of the insect world. Virulence 11: 238-246, 2020.

Shia AK, Glittenberg M, Thompson G, Weber AN, Reichhart JM, Ligoxygakis P. Toll-dependent antimicrobial responses in *Drosophila* larval fat body require Spätzle secreted by haemocytes. J. Cell Sci. 122: 4505-4515, 2009.

Trenczek T. Biological mediators of insect immunity. Annu. Rev. Entomol.: 42: 611-643, 1997.

Valgas C, de Souza SM, Smênia EFA, Smênia A Jr. Screening method to determine antibacterial activity of natural products. Braz. J. Microbiol. 38: 369-380, 2007.

Veeramani V, Sakthivelkumar S, Chitra S, Janarthanan S. Purification, characterization, and analysis of antibacterial activity of a serum lectin from the grub of rhinoceros beetle, *Oryctes rhinoceros*. Process Biochem. 53: 232-244, 2017.

Wessel N, Rousseau S, Caisey X, Quiniou F, Acksha F. Investigating the relationship between embryotoxic and genotoxic effects of benzo[*a*]pyrene, 17α-ethinylestradiol and endosulfan on *Crassostrea gigas* embryos. Aquat. Toxicol. 85: 133-142, 2007.

Wu G, Yi Y. Effects of dietary heavy metals on the immune and antioxidant systems of *Galleria mellonella* larvae. Comp. Biochem. Physiol. C Toxicol. Pharmacol. 167: 131-139, 2015.

Yamashita M, Iwabuchi K. *Bombyx mori* prohaemocyte division and differentiation in individual microcultures. J. Insect Physiol. 47: 325-331, 2001.

Yeaman MR, Yount NY. Mechanisms of antimicrobial peptide action and resistance. Pharmacol. Rev. 55: 27-55, 2003.

Zhang X, Zhang K. Cellular response to bacterial infection in the grasshopper *Oxya chinensis*. Biol. Open 8: bio045864, 1-10, 2019.